

## **Preparation and characterization of polycaprolactone microspheres by electrospaying**

Feng-Lei Zhou<sup>1,2,\*</sup>, Penny L. Hubbard Cristinacce<sup>3</sup>, Stephen J. Eichhorn<sup>4</sup> and Geoff J. M. Parker<sup>1,5\*</sup>

<sup>1</sup>Centre for Imaging Sciences, The University of Manchester, Manchester M13 9PT, United

Kingdom, <sup>2</sup>The School of Materials, The University of Manchester, Manchester M13 9PL, United

Kingdom, <sup>3</sup>School of Psychological Sciences, The University of Manchester, Manchester M13 9PT,

United Kingdom, <sup>4</sup>College of Engineering, Mathematics and Physical Sciences, North Park Road,

University of Exeter, Exeter EX4 4QF, United Kingdom, <sup>5</sup>Bioxydyn Limited, Rutherford House,

Manchester Science Park, Pencroft Way, Manchester M15 6SZ, United Kingdom.

\*Corresponding authors

Tel: +44 (0)161 275 5731; Fax: +44 (0)161 275 5145; Emails: geoff.parker@manchester.ac.uk and

fenglei.zhou@manchester.ac.uk

**Running title:** Electrospaying of 3D polycaprolactone microspheres

**Keywords:** Electrospaying, polycaprolactone, microspheres, 3D microstructure

### **Abstract**

The ability to reproducibly produce and effectively collect electrospayed polymeric microspheres with controlled morphology and size in bulk form is challenging. In this study, microparticles were produced by electrospaying polycaprolactone (PCL) of various molecular weights and solution concentrations in chloroform, and by collecting materials on different substrates. The resultant PCL microparticles were characterized by optical and electron microscopy to investigate the effect of molecular weight, solution concentration, applied voltage, working distance and flow rate on their morphology and size. The work demonstrates the key role of a moderate molecular weight and/or solution concentration in the formation of spherical PCL particles via an electrospaying process. Increasing the applied voltage was found to produce smaller and more uniform PCL microparticles. There was a relatively low increase in the particle average size with an increase in the working distance and flow rate. Four types of substrates were adopted to collect electrospayed PCL particles: a glass slide, aluminium foil, liquid bath and copper wire. Unlike 2D bulk structures collected on the other substrates, a 3D tubular structure of microspheres was formed on the copper wire and could find application in the construction of 3D tumour mimics.

### **1. Introduction**

Electrospaying and its variant, electrospinning, are two techniques capable of fabricating nano- or micro-sized droplets/fibres from polymer solutions by means of electric forces (Li and Xia 2004; Jaworek 2007). Electrospaying/electrospinning can be used to engineer micro- or nanometer

architectures such as particles, fibres, prints/fabrics or encapsulated particles with controllable nanostructure. Electrospaying/electrospinning parameters (applied voltage, flow rate, working distance, *etc.*), solution properties (solution viscosity, solution conductivity, surface tension, molecular weight of the polymer, *etc.*), and environmental conditions (temperature, humidity, *etc.*) are the main factors that influence the electrospaying/electrospinning process. By changing these factors, polymeric particles/fibres with various morphologies and sizes can be tuned for a specific polymer solution. Compared with the wide range of applications for electrospun fibres (Burger et al. 2006), electrospayed polymeric particles within the micro- to nano-meter range find applications mainly in drug delivery (Bock et al. 2012) .

Polycaprolactone (PCL) is suitable for long-term controlled drug delivery due to its high permeability to excipients, excellent biocompatibility, its ability to be fully excreted from the body and its slow degradation (more than one year) (Woodruff and Hutmacher 2010). There have been significant recent studies on the electrospinning of PCL because of the advantages of using this material for tissue scaffolds (Cipitria et al. 2011; Van der Schueren et al 2011). Compared with poly(lactic-co-glycolic acid) (PLGA), which is the most commonly used polymer in electrospaying (Bock et al. 2012) , there have been a relatively limited number of studies on the electrospaying of PCL (Wu and Clark 2007; Enayati et al. 2010, Bock et al. 2011; Guarino et al. 2012). In addition, although the effect of collecting substrates on the physical properties of electrospun nanofibres has been undertaken (Teo and Ramakrishna 2006), no previous reports on the effect of collecting substrates on electrospayed particle assemblies has been identified. Such information is important for the production of PCL microparticle assemblies with controlled morphology and size. This paper focuses on the electrospaying of PCL microparticles onto various collecting substrates. A systematic investigation on the effect of processing parameters, including polymer molecular weight, solution concentration, applied voltage, working distance and flow rate on the size of PCL particles produced was carried out. A number of different substrates were employed to collect PCL microparticles in order to produce various types of assemblies.

## **2. Experimental Section**

### *2.1. Materials*

Polycaprolactone in three formulations (PCL, number-average molecular weights  $M_n = 70,000\text{--}90,000$  (PCL-1), 45,000 (PCL-2) and 10,000 (PCL-3)  $\text{g mol}^{-1}$ ) was obtained from Sigma

Aldrich (Dorset, UK) and used as received. Chloroform solvent was also purchased from Sigma Aldrich (Dorset, UK).

## 2.2. Preparation of PCL microparticles

PCL solutions were prepared by dissolving PCL in chloroform and stirring overnight at room temperature. PCL microparticles were fabricated by an electrospaying process (**Fig. 1**) using a setup described previously for electrospinning (Zhou et al. 2011). Briefly, a high-voltage power supply (Glassman High Voltage, Model No. PS/FC30R04.0–22) was employed to tune the applied voltage between 0 and 30 kV. A 10 mL plastic syringe with a stainless-steel needle (inner diameter 1.19 mm) mounted on a syringe pump (SP230IWZ, World Precision Instruments) was used to feed PCL solution to the needle tip with a controllable feed rate. The fabricated particles were then collected on a grounded collector. All experiments were conducted in a fume cupboard under ambient conditions. The influence of a number of parameters on the physical properties of microparticles were studied, including PCL molecular weight, PCL concentration, applied voltage, flow rate and collector type. For the collector types a standard microscope glass slide, a flat sheet of aluminium foil, a water bath in a 50 mL beaker at room temperature and a custom-made spring-shaped copper wire (wire diameter - ~1.2 mm, length - ~100 mm, pitch - ~50 mm and outer diameter - ~75 mm) were used. All collectors were placed on a grounded aluminium plate (10 cm × 20cm) located below the spinneret.

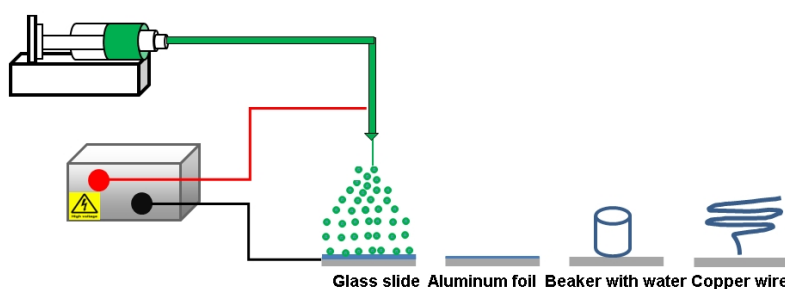


**Figure 1.** Schematic of the electrospaying process with various collectors (not scaled).

## 2.3. Optical and scanning electron imaging

The morphology of the surface of electrospayed particles was observed using an Olympus BH2-UMA optical microscope and a Philips XL30 FEG SEM or a Phenom G2 pro desktop Scanning Electron Microscope (SEM) with an accelerating voltage of 5 kV. In order to determine the size of the electrospayed particles, a glass slide was introduced in the setup and held in contact with the collector, in the centre of the spraying zone for a few minutes. The electrospayed PCL particles collected on the aluminium foil were coated with a thin gold film to increase their conductivity before SEM imaging.

Image processing software ImageJ was used to measure particles' sizes from optical and SEM micrographs.

#### *2.4 Statistical analysis*

The statistical analysis was performed with the Origin Pro software. A value of  $p < 0.05$  was defined as statistically significant. One-way or two-way analysis of variance (ANOVA) followed by a Bonferroni multiple comparison test was used to analyse the particles' size data. One-way ANOVA was used to analyse applied voltage, working distance or flow rate when solution concentration was fixed. Two-way ANOVA was used to analyse the interaction of solution concentration with applied voltage, or working distance or flow rate on particle size.

### **3. Results and discussion**

It is important to stress that the variables involved in the electrospaying process are generally not independent in terms of their impact on particle size. In practice, these variables can be varied only within some finite range to obtain particles of desirable morphology and size and even their relationship with electrospayed particle sizes holds truly within an optimum range.

#### *3.1. Effect of polymer molecular weight*

For a polymer solution to be electrospayed to produce particles, or electrospun for fibres, there are a range of molecular chain entanglement regimes: dilute, semi-dilute unentangled and semi-dilute entangled. These regimes are determined by the polymer molecular weight and solution concentration. For electrospaying of spherical particles, the regime of choice is the semi-dilute entangled regime, where solid and reproducible particles can be produced (Bock et al. 2012). In terms of the electrospinning of smooth fibres, the concentration of the polymer solution has to be well above the semi-dilute entangled regime (Gupta et al. 2005). However, there have been some recent reports of electrospinning of nanofibres from non-polymeric materials, e.g. cyclodextrin (Celebioglu and Uyar 2011), where no polymer molecular entanglement was present but a high solution concentration/viscosity was still essential.

Solution PCL-1 was first electrospayed since it used a molecular weight that has been previously reported for the electrospinning of fibres (Cipitria et al. 2011). As shown in **Fig. 2a-b**, it was not possible to produce spherical particles from PCL-1 by electrospaying, even when reducing the solution concentration from 9 wt.%, where smooth PCL fibres were produced, to 0.5 wt.%, from which beaded PCL fibres were made. PCL particles were readily produced from a 9 wt.% PCL solution when

the molecular weight was decreased to 45k (PCL-2) and 10k (PCL-3); particles were produced with average diameters of  $36.2 \pm 2.8 \mu\text{m}$  and  $47.2 \pm 15.7 \mu\text{m}$ , respectively (**Fig. 2c-d**). When the concentration of PCL-2 was slightly increased from 9 wt.% to 11 wt.%, a number of very fine PCL fibres were produced, along with microparticles (see **Fig. 2e**). However, for PCL-3, particles with an average diameter of  $50.3 \pm 5.1 \mu\text{m}$  were produced, even from a 30 wt.% solution (**Fig. 2f**), indicating a low molecular weight of PCL could produce spherical particles from a wider range of solution concentrations. The effect of PCL molecular weight and solution concentration on the formation of particles is in agreement with similar findings for the electrospaying of PLGA (Meng et al. 2009). SEM imaging (inset in **Fig. 2c**) further revealed that the electrospayed PCL particles from PCL-2 had spherical shape and smooth surface. For PCL-3, the particles appeared to collapse when the PCL concentration was 9 wt.% (inset in **Fig. 2d**). A hole with an average size of approximately  $8.4 \pm 2.3 \mu\text{m}$  was however formed on each particle surface when the PCL concentration was increased to 30 wt.% (inset in **Fig. 2f**). It has been previously reported that the surface morphology of PCL particles changes from a smooth surface to a rough corrugated surface when the solution concentration is reduced and that a lower molecular weight leads to the formation of particles with a hole in the surface (Xie et al. 2006). A solvent evaporation-induced phase separation was proposed to explain the formation of holes in electrospayed PCL particles (Wu and Clark 2007).

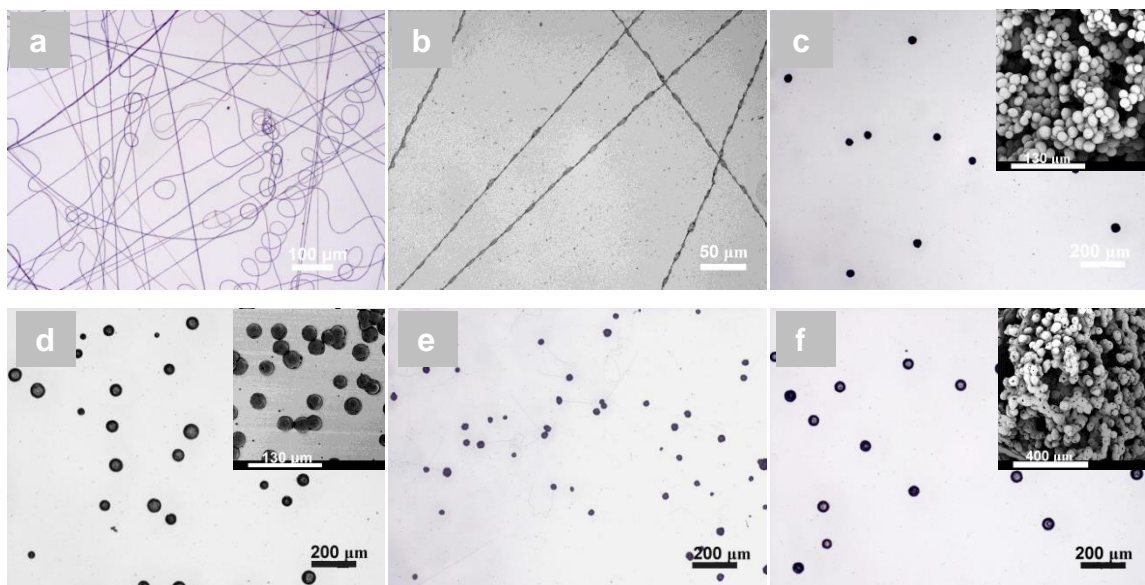


**Figure 2.** Optical micrographs showing the effects of polymer molecular weight and solution concentration on electrospayed fibres and particles: (a) smooth fibres from PCL-1, 10 wt.%; (b) beaded fibres from PCL-1, 0.5 wt.%; (c) particles from PCL-2, 9 wt.% (average diameter  $\pm$  standard deviation:  $36.2 \pm 2.8 \mu\text{m}$ , inset: SEM micrograph); (d) particles from PCL-3, 9 wt.% ( $47.2 \pm 15.7 \mu\text{m}$ , inset: SEM micrograph); (e) particles from PCL-2, 11 wt.%; (f) particles from PCL-3, 30 wt.% ( $50.3 \pm 5.1 \mu\text{m}$ , inset: SEM micrograph).

inset: SEM micrograph); (e) particles with fibrils from PCL-2, 11 wt. %; (f) particles from PCL-2, 30 wt.% ( $50.3 \pm 5.1 \mu\text{m}$ , inset: SEM micrograph).

### 3.2. Effect of applied voltage

A sufficient applied voltage is required to overcome the surface tension of the droplet at the needle tip and thus controls the morphology and size of electrosprayed particles. It is generally accepted that an increase in the applied voltage can lead to a decrease in the size of microparticles. However, very high voltages cannot be used because of the onset of an unstable jet. There is usually a lower and upper voltage limit, which allows a stable jet in electrospraying, resulting in monodispersed particles and better repeatability and reproducibility.

For PCL-2 with 1 wt.% and 5 wt.% concentrations, an increase in applied voltage tended to produce more uniform and smaller PCL particles (**Fig. 3a-c**). For example, in the case of 1 wt.% PCL-2 solution, the average diameter of the particles significantly increased (one-way ANOVA,  $p < 0.05$ ) from  $16.9 \pm 5.9 \mu\text{m}$  at 6.5 kV to  $18.6 \pm 7.6 \mu\text{m}$  at 7.5 kV, and then dramatically decreased to  $10.0 \pm 1.6 \mu\text{m}$  at 8.5 kV (**Table 1**). There were also significant changes in particle diameters for a 5 wt.% PCL solution ; from  $27.6 \pm 11.4 \mu\text{m}$  through  $23.8 \pm 6.8 \mu\text{m}$ , to  $21.9 \pm 5.6 \mu\text{m}$  (**Fig. 3d-f**) with increasing applied voltage. These dramatic reductions in diameter are likely to be because the stronger electric field at the higher voltage forces the conical meniscus at the needle tip to deform and to break into smaller droplets. As shown in **Fig. 3g-i**, for a 7 wt.% PCL solution, the change in PCL particle sizes became much less noticeable than those from 1 wt.% and 5 wt.% solutions. Bonferroni-corrected post-hoc tests further pointed towards no significant difference ( $p > 0.05$ ) in the mean sizes of particles produced from a 7 wt.% PCL-2 solution when the applied voltage was changed from 9 kV to 10 kV, although there was a significant change from 8 kV to 9 kV. This indicated that the effect of the applied voltage could become weak with a relatively high concentration of the solution. It should be noted that too a high voltage resulted in an unstable spray (data not shown). Two-way ANOVA tests further revealed that the solution concentration and applied voltage had a significant interaction ( $p < 0.05$ ). As shown by the histograms in **Table 1**, PCL particles produced using 1 wt.% and 5 wt.% solutions had wider size distributions than those generated from 7 wt.% solution; for all three PCL solutions, a higher applied voltage could benefit the formation of uniform spherical particles.

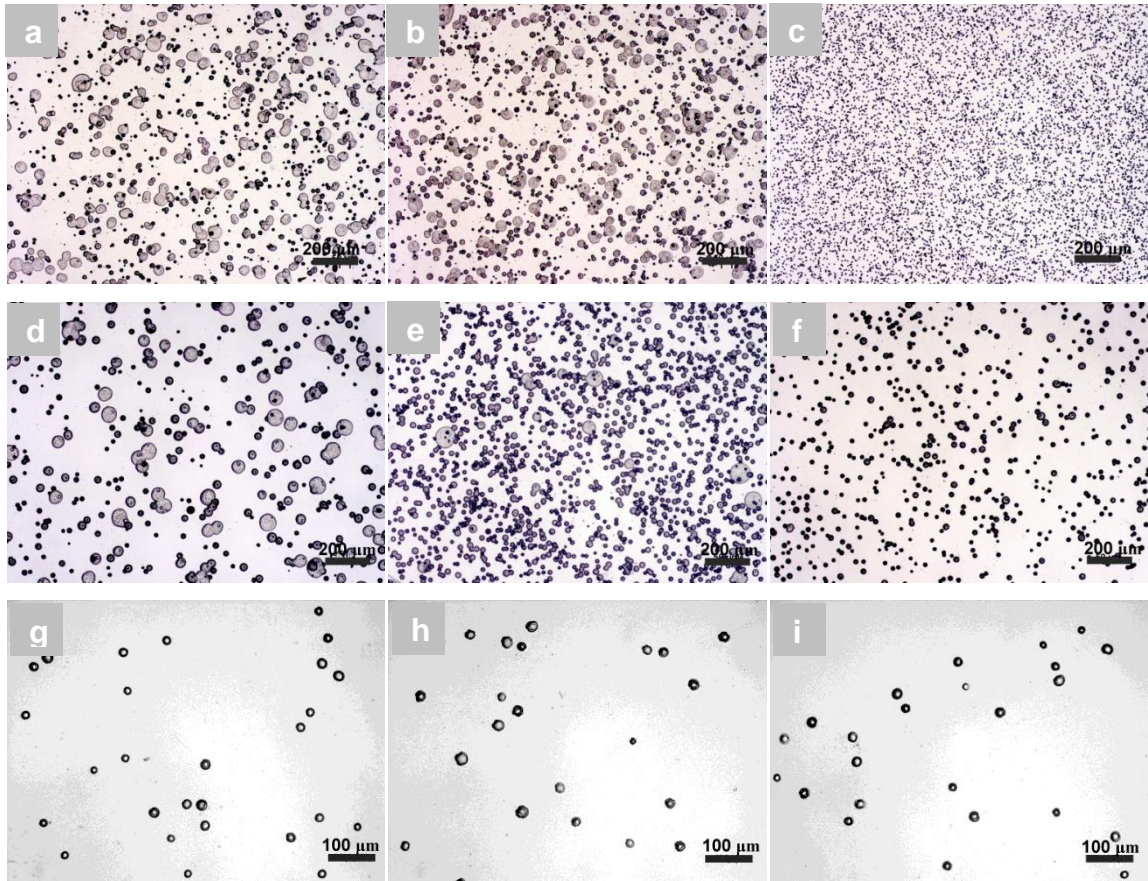


**Figure 3.** Effect of applied voltage on the morphology and size of PCL particles electrospayed from PCL-2,  $M_w = 45k$ . (a) 1 wt.%-6.5 kV; (b) 1 wt.%-7.5 kV; (c) 1 wt.%-8.5 kV; (d) 5 wt.%-6.5 kV; (e) 5 wt.%-7.5 kV; (f) 5 wt.%-8.5 kV; (g) 7 wt.%-8 kV; (h) 7 wt.%-9 kV; (i) 7 wt.%-10 kV.

**Table 1.** Mean and standard deviation of diameters and distributions of PCL particles produced under different applied voltages.

Applied voltage Solution concentration $d_p$ ( $\mu\text{m}$ )	6.5 kV	7.5 kV	8.5 kV	Particle diameter distributions
1 wt. %	$16.9 \pm 5.9$ $\mu\text{m}$	$18.6 \pm 7.6$ $\mu\text{m}$	$10.0 \pm 1.6$ $\mu\text{m}$	
5 wt. %	$27.6 \pm 11.4$ $\mu\text{m}$	$23.8 \pm 6.8$ $\mu\text{m}$	$21.9 \pm 5.6$ $\mu\text{m}$	
7 wt. % *	$18.7 \pm 2.4$ $\mu\text{m}$	$21.1 \pm 3.0$ $\mu\text{m}$	$19.3 \pm 2.6$ $\mu\text{m}$	

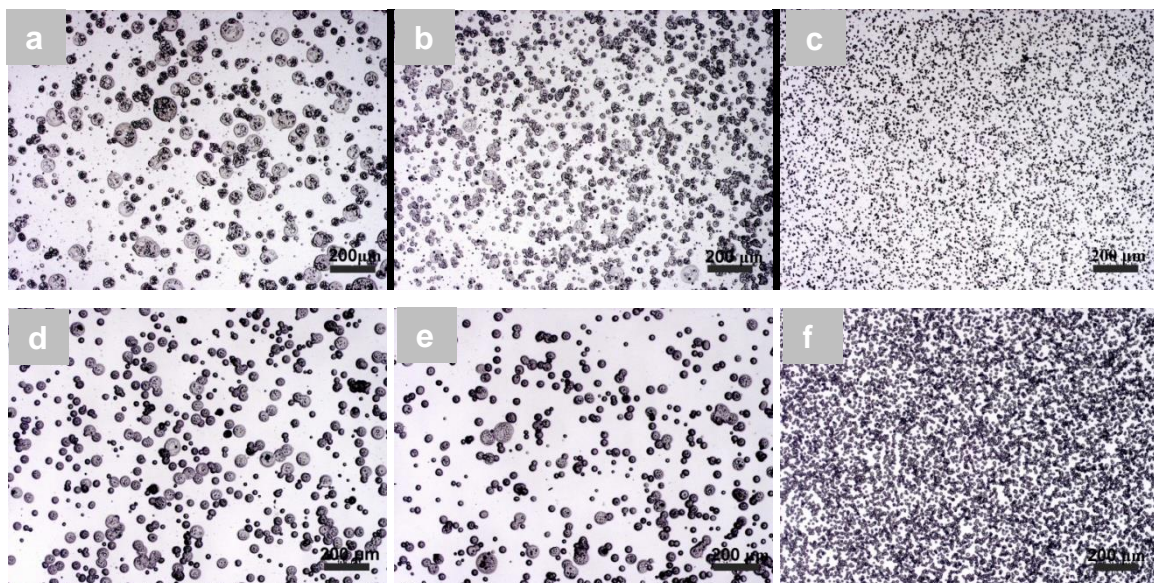
\* for the 7 wt.% PCL solutions, the applied voltages were 8 kV, 9 kV and 10 kV. The relationship between sphere sizes and applied voltage/solution concentration was also plotted using  $x$ - $y$ - $z$  spatial coordinates. These plots were included as supplementary material.

For PCL-3 with concentrations of 1 wt.% and 5 wt.%, higher applied voltages also produced more uniform (as shown by the size distributions in Table 2) and spherical particles with smaller diameters



(**Fig. 4a-c**). For example, there were significant decreases in particle diameter from  $27.0 \pm 9.9 \mu\text{m}$  to  $10.4 \pm 2.1 \mu\text{m}$  and from  $31.2 \pm 13.8 \mu\text{m}$  to  $13.9 \pm 4.7 \mu\text{m}$  (**Fig. 4d-f**), respectively, when the applied voltage was varied from 6.5 kV to 8.5 kV. When the solution concentration was increased to 9 wt.%, it is also noted that when the applied voltage was increased, a dramatic decrease in the particle diameter occurred (from  $53.4 \pm 17.6 \mu\text{m}$  to  $18.7 \pm 5.3 \mu\text{m}$ ) (**Fig. 4g-i**). This observation is consistent with previous findings. However, Bonferroni post-hoc tests showed no significant changes in mean particle diameter (from  $31.2 \pm 13.8 \mu\text{m}$  to  $30.0 \pm 12.7 \mu\text{m}$ ) occurred at a 5 wt.% concentration when the voltage was changed from 6.5 kV to 7.5 kV. Two-way ANOVA showed there is a significant relationship between solution concentration and applied voltage ( $p < 0.05$ ). **Table 2** shows the size distributions of particles from the solutions with different concentrations. Clearly, PCL particles produced at a lower applied voltage have broader size distributions and larger average sizes than those formed at higher applied voltages, especially for PCL solutions with 1 wt. % and 5 wt. % concentrations.

From these results it can be seen that a relatively higher applied voltage was required to produce PCL particles with uniform size, particularly for low concentration solutions of low molecular weight PCL. However, it is worth mentioning that for a given solution concentration, the range of applied voltage for a stable electro spraying process was typically narrow and mainly influenced by flow rate. In the electro spraying process, applied voltage may affect several factors including electrostatic force on polymer solution droplet, polymer mass fed out from a tip of needle, etc. A balance between these factors may determine the final morphology and size of electro sprayed particles.



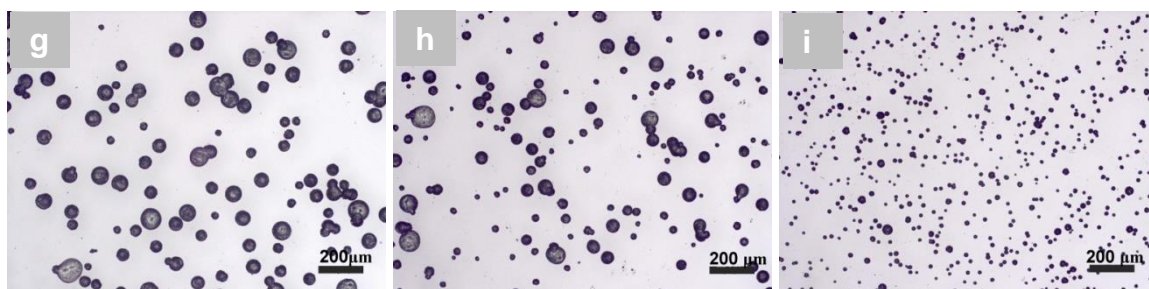
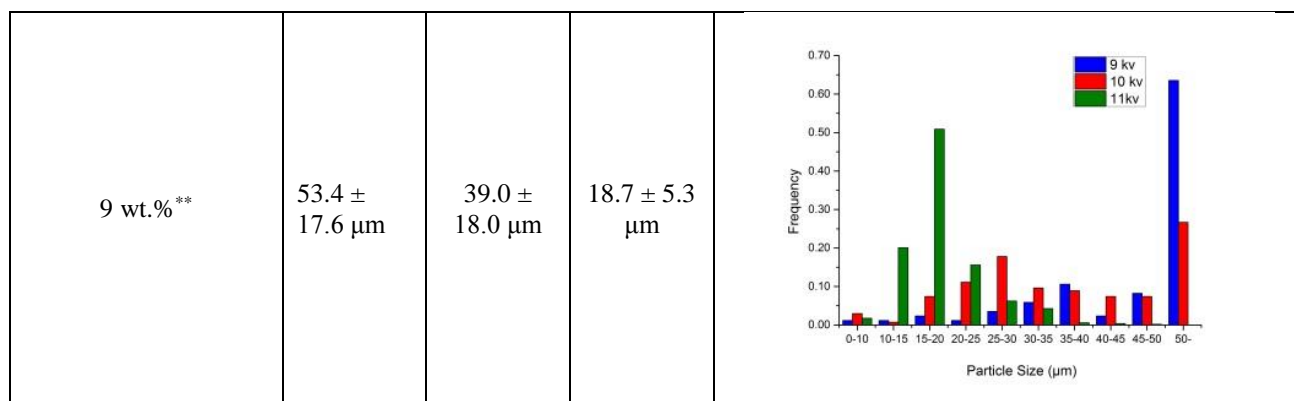


**Figure 4.** Effect of applied voltage on the morphology and size of PCL particles electrospayed from PCL-3 solution,  $M_w = 10k$ . (a) 1 wt.%-6.5 kV; (b) 1 wt.%-7.5 kV; (c) 1 wt.%-8.5 kV ; (d) 5 wt.%-6.5 kV ; (e) 5 wt.%-7.5 kV ; (f) 5 wt.%-8.5 kV ; (g) 9 wt.%-9 kV ; (h) 9 wt.%-10 kV ; (i) 9 wt.%-11 kV.

**Table 2.** Mean and standard deviations of PCL particle diameters and their distributions, produced under different applied voltages.

Applied voltage Solution concentration $d_p$ ( $\mu m$ )	6.5 kV	7.5 kV	8.5 kV	Particles diameter distributions
1 wt.%	$27.0 \pm 9.9 \mu m$	$18.9 \pm 7.0 \mu m$	$10.4 \pm 2.1 \mu m$	
5 wt.%	$31.2 \pm 13.8 \mu m$	$30.0 \pm 12.7 \mu m$	$13.9 \pm 4.7 \mu m$	



\*\* for the 9 wt.% PCL solution, the applied voltages were 9 kV, 10 kV and 11 kV. The relationship between sphere sizes and applied voltage/solution concentration was also plotted using  $x$ - $y$ - $z$  spatial coordinates. These plots were included as supplementary material.

### 3.3. Effect of working distance

The working distance in the electrospaying process is the distance from the needle tip of the spinneret to the grounded collector. This distance determines the time that the solvent can take to evaporate when an electrospayed droplet accelerates towards the grounded collector. An increase in the working distance reduces the electric field strength but increases the travel time of droplets, which has an effect on the evaporation of the solvent. Therefore, it could have a dual effect on the resultant electrospayed particles, up to a point at which a particular factor may become dominant. It was noted that PCL particles tended to merge with neighbouring particles due to the presence of residual solvent when the working distance was too short (for example < 10 cm). However, a working distance greater than 30 cm could lead to a significant loss of particles to the surroundings as they travel to the nearest grounded object in order to discharge. Therefore, similar to previous studies on electrospaying of polystyrene (Park and Lee 2009) and chitosan (Arya et al. 2009), the working distance had to be optimized to ensure the sufficient evaporation of any remaining solvent in the PCL particles, thus alleviating their merging, and appropriate collection efficiency.

Uniformly sized spherical particles were difficult to produce using a 1 wt.% PCL-2 solution, particularly when using a 10 cm working distance (**Fig. 5a**). Increasing the working distance at this solution concentration improved the size uniformity and reduced the presence of larger particles (**Fig. 5b-c**). There were significant changes ( $p < 0.05$ ) in the mean particle diameters from  $18.6 \pm 7.6 \mu\text{m}$ , through  $20.8 \pm 5.7 \mu\text{m}$  to  $27.6 \pm 9.5 \mu\text{m}$  for a 1 wt.% PCL solution (**Table 3**). When 5 wt.% and 7 wt. % PCL-2 solutions were used, spherical PCL particles were produced at all three working distances (**Fig.**

**5d-f and Fig. 5g-i).** At first, there was no significant change in diameter from  $23.8 \pm 6.8 \mu\text{m}$  to  $24.3 \pm 6.6 \mu\text{m}$  ( $p > 0.05$ ) and then a significant increase ( $p < 0.05$ ) to  $26.3 \pm 6.2 \mu\text{m}$  with the increasing working distance at 5 wt.% concentration. In the case of 7 wt.% PCL solution, particle sizes increased significantly ( $p < 0.05$ ) from  $21.1 \pm 3.0 \mu\text{m}$  to  $28.0 \pm 4.2 \mu\text{m}$ , and then increased less significantly ( $p > 0.05$ ) to  $30.0 \pm 7.1 \mu\text{m}$  when the working distance was varied between 15 cm and 20 cm. Two-way ANOVA showed a significant relationship ( $p < 0.05$ ) between the solution concentration and working distance. The histograms in **Table 3** reveal the size distributions of PCL particles from 1 wt.%, 5 wt.% and 7 wt. % PCL-2 solutions. Particles with diameters exceeding  $40 \mu\text{m}$  were present for 1 wt.% and 5 wt.% PCL solutions. PCL particles electrospayed from a 7 wt.% PCL solution had a relatively narrow diameter distribution, centralized around 20-25  $\mu\text{m}$  and 25-30  $\mu\text{m}$  for 15 cm and 17.5 cm working distances, respectively. For the particles produced using a working distance of 20 cm, the particle percentage in the range of 25-30  $\mu\text{m}$  was similar to that in the range of 30-35  $\mu\text{m}$ .

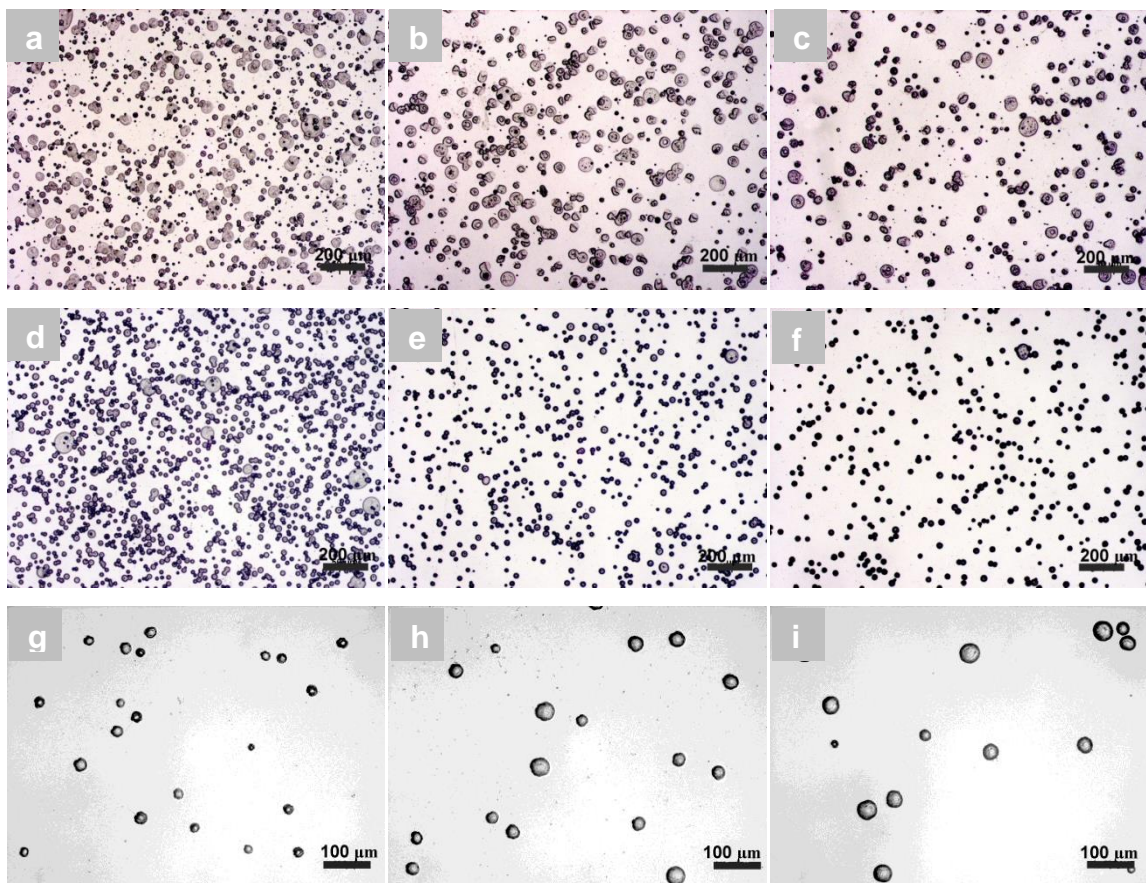


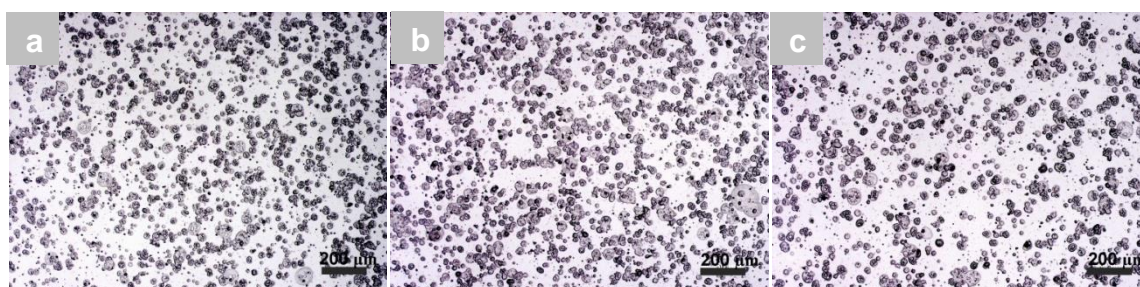
**Figure 5.** Effect of working distance on the morphology and size of PCL particles electrospayed from PCL-2. (a) 1wt.%-10 cm; (b) 1wt.%-12.5 cm; (c) 1wt.%-15 cm; (d) 5wt.%-10 cm; (e) 5wt.%-12.5 cm; (f) 5wt.%-15 cm; (g) 7wt.%-15 cm; (h) 7wt.%-17.5 cm; (i) 7wt.%-20 cm.

**Table 3.** Mean and standard deviations of PCL particle diameters and their distributions produced under different working distances.

Working distance $d_w$ (μm) Solution concentration	10 cm	12.5 cm	15 cm	Particles diameter distributions
1 wt.%	$18.6 \pm 7.6$ μm	$20.8 \pm 5.7$ μm	$27.6 \pm 9.5$ μm	
5 wt.%	$23.8 \pm 6.8$ μm	$24.3 \pm 6.6$ μm	$26.3 \pm 6.2$ μm	
7 wt.% <sup>***</sup>	$21.1 \pm 3.0$ μm	$28.0 \pm 4.2$ μm	$30.0 \pm 7.1$ μm	

\*\*\* for the 7 wt.% PCL solution, the working distance was 15 cm, 17.5 cm and 20 cm. The relationship between sphere sizes and working distance/solution concentration was also plotted using  $x$ - $y$ - $z$  spatial coordinates. These plots were included as supplementary material.

For the PCL-3 solution with a 1 wt.% concentration, when the working distance was varied from 10 cm to 15 cm, it was observed that the cone-jet was not stable, resulting in PCL particles with polydisperse sizes (average diameters were  $\sim 20 \mu\text{m}$ ); no significant change ( $p > 0.05$ ) in PCL particle average sizes was however observed, as shown in **Fig. 6a-c**, indicating that working distance was not as influential as for the 1 wt.% PCL-2 solution. When the PCL concentration was increased to 5 wt.%, the electrospaying jet became stable, resulting in less polydisperse particle sizes; the diameters of resultant particles however changed significantly ( $p < 0.05$ ) from  $30.0 \pm 12.7 \mu\text{m}$  to  $34.2 \pm 12.8 \mu\text{m}$  with an increase in the working distance from 10 cm to 12.5 cm, but did not change significantly ( $35.8 \pm 8.0 \mu\text{m}$ ;  $p > 0.05$ ) with an increase in the working distance to 15 cm (**Fig. 6d-f**). When the PCL concentration was increased to 9 wt.%, there were noticeable increases (ANOVA,  $p < 0.05$ ) in the mean particle diameter from  $33.6 \pm 17.3 \mu\text{m}$ , through  $39.0 \pm 18.0 \mu\text{m}$ , to  $54.3 \pm 15.8 \mu\text{m}$  when the working distance was increased from 17.5 cm to 25 cm (**Fig. 6g-i**). Two-way ANOVA showed significant interactions ( $p < 0.05$ ) between solution concentration and working distance. **Table 4** shows the size distributions of electrospayed particles from a PCL-3 solution with 1 wt.%, 5 wt.% and 9 wt.% concentrations. There were no particles with diameters larger than  $50 \mu\text{m}$  produced from 1 wt.% solution. Such PCL particles were present for a 5 wt.% solution and became more apparent ( $\sim 60 \text{ wt.}\%$ ) in the case of a 9 wt.% solution. In addition, for the 5 wt. % and 9 wt.% solutions, with an increase in the working distance, PCL particles became more uniform. For example, around 40% of the particles had diameters in the range  $35\text{-}40 \mu\text{m}$  at a working distance of 15 cm for a 5 wt.% solution but many fewer particles were in that range at both 10 cm and 12.5 cm working distances. For a 9 wt.% solution, 60% of the particles were larger than  $50 \mu\text{m}$  when the working distance was increased to 25 cm from 15 cm. In this case particles sizes also varied significantly.



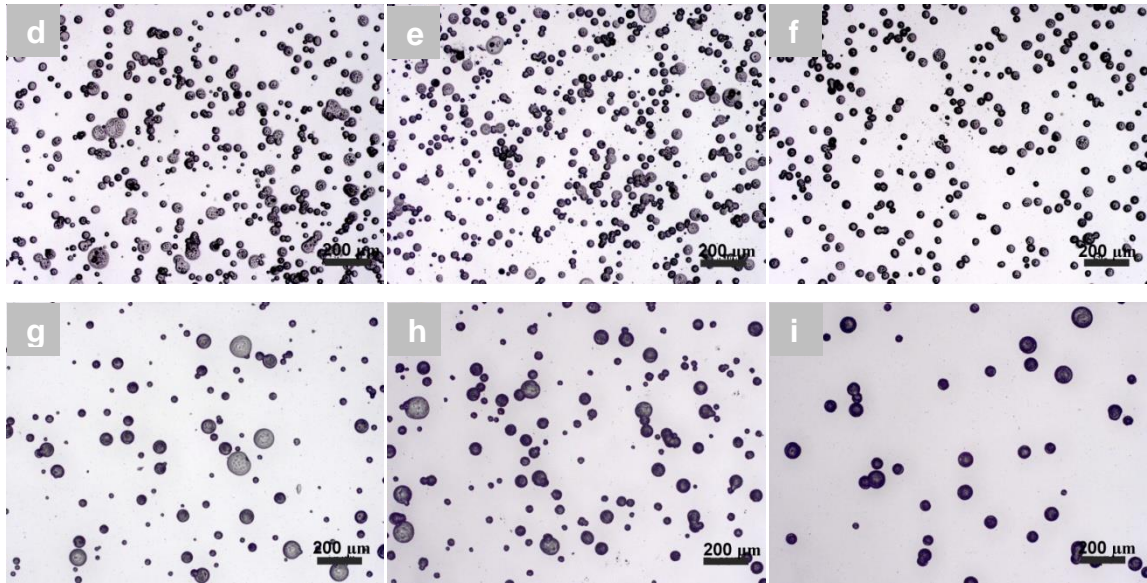


**Figure 6.** Effect of working distance on the morphology and size of PCL particles electrospayed from PCL-3. (a) 1 wt.%-10 cm; (b) 1 wt.%-12.5 cm; (c) 1 wt.%-15 cm; (d) 5 wt.%-10 cm; (e) 5 wt.%-12.5 cm; (f) 5 wt.%-15 cm; (g) 9 wt.%-15 cm; (h) 9 wt.%-20 cm; (i) 9 wt.%-25 cm.

**Table 4.** Mean and standard deviation of diameters of PCL particles and their distributions produced under different working distances.

Working distance $d_s$ ( $\mu\text{m}$ ) Solution concentration	10 cm	12.5 cm	15 cm	Particles diameter distributions

1 wt.%	$18.9 \pm 7.0$ $\mu\text{m}$	$20.1 \pm 6.4$ $\mu\text{m}$	$20.6 \pm 9.0$ $\mu\text{m}$	
5 wt.%	$30.0 \pm 12.7$ $\mu\text{m}$	$34.2 \pm 12.9$ $\mu\text{m}$	$35.8 \pm 8.0$ $\mu\text{m}$	
9 wt.% ****	$33.6 \pm 17.3$ $\mu\text{m}$	$39.0 \pm 18.0$ $\mu\text{m}$	$54.3 \pm 15.8$ $\mu\text{m}$	

\*\*\*\*for the 9 wt.% PCL solutions, the working distance were 15 cm, 20 cm and 25 cm. The relationship between sphere sizes and working distance/solution concentration was also plotted using  $x$ - $y$ - $z$  spatial coordinates. These plots were included as supplementary material.

In general, larger PCL particles were generated with longer working distances, which was consistent with the trend observed for the electrospaying of poly lactide-co-glycolide (PLGA) (Yao et al. 2008). However, it was also reported that the size of electrospayed chitosan particles first increased and then decreased with an increasing working distance (Arya et al. 2009). A large working distance tended to produce particles with a spherical shape and a narrow size distribution, especially for a high concentration solution. This could be due to the fact that by increasing the working distance the polymer chains to have sufficient time to diffuse within the droplet and thus reduce polydispersity



(Bock et al. 2012). It was also found that the effect of working distance on particle sizes became less significant for PCL-2 solutions but more significant for PCL-3 solutions with increasing concentration. This could be caused by the higher level molecular entanglement in PCL-2 than PCL-1, which restricts polymer chain diffusion.

### 3.4. Effect of flow rate

In the electrospaying/electrospinning process, a voltage–flow rate operating diagram is usually used to describe the jet behaviour (Hohman et al. 2001; Hohman et al.2001; Guarino 2012). There is typically a stability window within which a steady cone-jet can form. It is well-known that the average sizes of electrospayed particles increase with an increasing solution flow rate (Bock et al. 2011). In this study, 5 wt.% PCL-2 and 9 wt.% PCL-3 solutions were used to prepare particles under varying flow rates. The resultant particles from those solutions are shown in **Fig. 7a-c** and **Fig. 7d-f**, respectively. It can be seen that particles from the 9 wt.% PCL-3 solution were much larger than those from 5 wt.% PCL-2. The mean diameter of PCL particles increased significantly ( $p < 0.05$ ) from  $18.0 \pm 5.0 \mu\text{m}$  to  $29.7 \pm 9.6 \mu\text{m}$  (**Table 5**) and from  $32.2 \pm 15.0 \mu\text{m}$  to  $41.1 \pm 17.1 \mu\text{m}$  when flow rate was varied from  $5 \mu\text{L min}^{-1}$  to  $15 \mu\text{L min}^{-1}$  and from  $2 \mu\text{L min}^{-1}$  to  $10 \mu\text{L min}^{-1}$ , respectively. Interestingly, Bonferroni-corrected post-hoc tests found that the former increase in flow rate resulted in a more significant change in particle size than the latter for both PCL-2 and PCL-3 solutions. This indicates that particle sizes could be more effectively controlled by the flow rate when it is varied from the lower limit of the stability window. Additionally, the size of particles from a 5 wt.% (PCL-2) solution was more uniform when a low flow rate was used (**Fig. 7g**); the sizes of all particles produced from a 9 wt.% PCL-3 solution had a large variability with a changing flow rate (**Fig. 7h**).

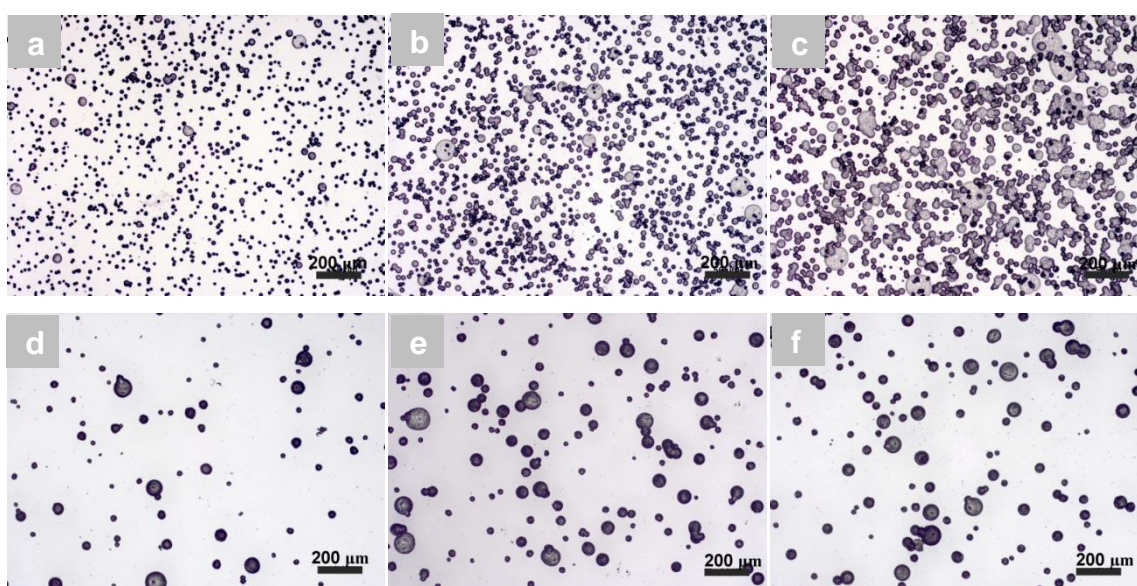


**Figure 7.** Effect of flow rate on the morphology and size of PCL particles. (a) PCL-2-5 wt.%- 0.3 mL h<sup>-1</sup> ; (b) PCL-2-5 wt.%-0.6 mL h<sup>-1</sup>; (c) PCL-2-5 wt.%- 0.9 μL min<sup>-1</sup>; (d) PCL-3-9 wt.%-0.12 mL h<sup>-1</sup>; (e) PCL-3-9 wt.%-0.36 mL h<sup>-1</sup>; (f) PCL-3-9 wt.%- 0.6 mL h<sup>-1</sup>

**Table 5.** Mean PCL particle diameter and standard deviation and their distributions produced under different flow rates.

Flow rate Solution concentration $d_p$ (μm)	0.3 mL h <sup>-1</sup>	0.6 mL h <sup>-1</sup>	0.9 mL h <sup>-1</sup>	Particle diameter distributions
5 wt.%	18.0 ± 5.0 μm	23.8 ± 6.8 μm	29.7 ± 9.6 μm	
9 wt.%	32.2 ± 15.0 μm	39.0 ± 17.9 μm	41.1 ± 17.1 μm	

Note: the relationship between sphere sizes and flow rate/solution concentration was also plotted using *x-y-z* spatial coordinates. These plots were included as supplementary material.

### 3.5. Effect of particle collector

In a typical electro spraying process, a solid, electrically conducting substrate (usually a grounded electrode) is used to collect particles. In a study (Wu and Clark 2007), a water bath was used to collect PCL particles electro sprayed from PCL/chloroform, resulting in a porous surface to the particles. Here four different types of collectors including a glass slide, aluminium foil, water bath and a spring-shaped

copper wire were employed to collect PCL particles from a 9 wt.% PCL-2 solution to study the deposited particles collected on these substrates. As shown in **Fig. 8a-c**, PCL particles on the glass slide and aluminium foil tended to stick together to form aggregates, especially after an extended electro spraying time. Moreover, it was also observed that only a small amount of particles could reach the surface of the grounded plate; this was especially true for long working distances. The majority of particles were found to be carried by the air flow, and finally deposit on other surfaces in the fume cupboard. Therefore, the collection efficiency of PCL particles onto a glass slide or aluminium foil was low. Similar observations on electro sprayed particle fusion and loss during collection was also reported for the electro spraying of chitosan (Arya et al. 2009).

Various collection systems, for example, a water bath and an air jet flow, have been introduced into the electro spraying process to avoid particle aggregation and improve collection rates (Xie et al. 2006; Xu and Hanna 2006). In the present study a water bath was also used to collect PCL particles. However, a film formed on the surface of the water bath (**Fig. 8d**), which hampered the dispersion of the particles. This was similar to a report on the deposition of electro spun PCL nanofibres in distilled water, where deposited material was found to float on the surface (Kostakova et al. 2014). In order to more efficiently capture the particles that are carried in the air flow of the fume hood, a grounded spring-shaped metal wire was placed in the spraying zone between the spinneret and the grounded plate. It was observed that the electro sprayed PCL particles were effectively attracted to and deposited on the grounded wire, which resulted in the formation of 3D tubular structure after an extended operation time (**Fig. 8e**). The electro spraying of 3D microparticles was a one-step process, compared to other 3D microparticle fabrication methods (Nukavarapu et al. 2008; Yu et al. 2015). The SEM micrographs in **Fig. 8 f-g** indicate that the collected particles on the surface of the copper wire had a smooth surface and a uniform size. However sphere packing tended to become denser from the outside to inside of the tubular structure, as shown in Fig. 8h.

Most recently, a number of novel spinnerets for the mass production of core-shell structured polymeric spheres/fibres have been reported (Sharma et al. 2012; Megdi et al. 2013; Vyslouzilova et al. 2014; Labbaf et al. 2014; Qin and Jiang 2014, Yan et al. 2015; Mahalingam et al. 2015) . It can be envisaged that 3D core-shell/hollow microspheres will be formed when such a collecting system is introduced into these processes. In future work we will explore in details these novel spinnerets to produce bulk structures with core-shell structured microfibrils/spheres which usually took us a few hours to prepare for their application in diffusion MRI (Hubbard et al. 2015; McHugh et al. 2015).

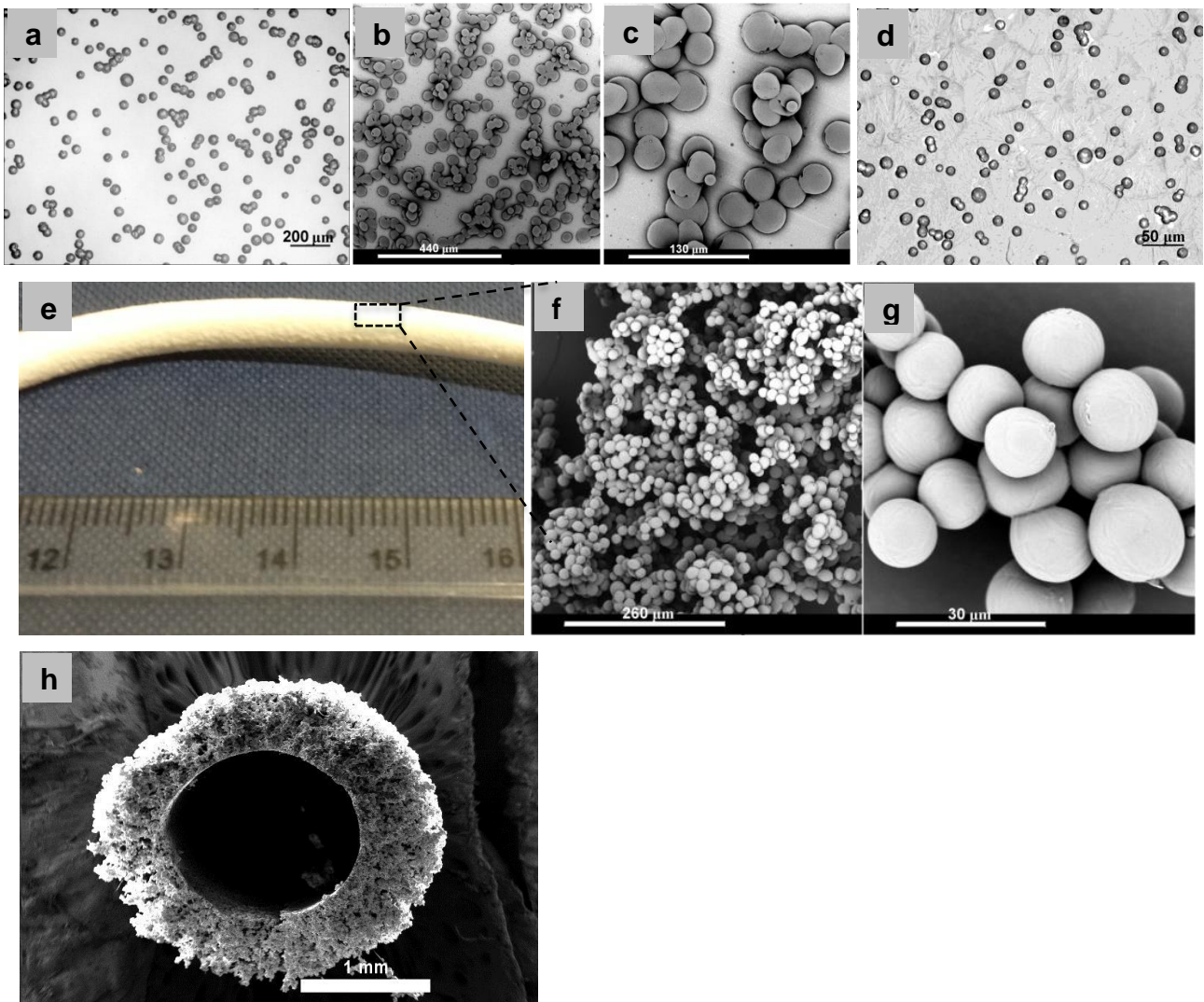


**Figure 8.** Optical and SEM micrographs of PCL particles electrospayed from 9 wt.% PCL-2 solution on different collectors. (a) glass slide; (b) aluminium foil; (c) close-up image of (b); (d) water bath; (e) digital image of tubular assembly of spheres on a copper wire; (f-h) SEM images with different magnifications of spheres in and cross-section of 3D tubular assembly.

#### 4. Conclusions

In summary, electrospaying was demonstrated to be a versatile method for generating PCL particles with controllable morphology, size and structure, which could be tuned with polymer molecular weight, solution concentration, applied voltage, flow rate, working distance and particle collector. It was observed that PCL molecular weight and solution concentration had a large effect on the formation and morphology of particles. Only microfibres were produced by electrospaying from PCL-1 ( $M_n = 70,000\text{--}90,000 \text{ g mol}^{-1}$ ) with 0.5 wt.% to 10 wt.% concentration. Microparticles were generated from both PCL-2 ( $45,000 \text{ g mol}^{-1}$ ) and PCL-3 ( $10,000 \text{ g mol}^{-1}$ ) solutions with various concentrations, the

latter having a wider range of possible concentrations. In order to avoid fiber formation, an increased polymer concentration must be coupled with a decreased molecular weight, ensuring electrospaying occur in the semidilute entangled regime, which leads to the formation of spherical and homogeneous particles. The morphology and size of the resultant particles were influenced to different extents by the applied voltage, working distance and flow rate, among of which the effect of applied voltage was most significant. There was however a narrow range of applied voltage allowing a more stable electrospaying process. PCL particles couldn't be collected in a water bath as efficiently as a grounded copper wire collecting substrate due to the particle aggregation on water surface. Furthermore, a 3D tubular assembly of smooth and spherical PCL microparticles could be formed on the copper wire and be used as a tumour cell mimic.

## Acknowledgement

The financial support received from the Cancer Research UK (CRUK) and Engineering and Physical Sciences Research Council (EPSRC) Cancer Imaging Centre in Cambridge and Manchester (C8742/A18097) is acknowledged.

## References

1. Arya, N., Chakraborty S., Dube, N., and Katti, D.S. (2009). Electrospaying: A facile technique for synthesis of chitosan-based micro/nanospheres for drug delivery applications. *J. Biomed. Mater. Res-B*, **88B**(1): 17-31.
2. Bock, N., Dargaville, T. R., and Woodruff, M. A. (2012). Electrospaying of polymers with therapeutic molecules: State of the art. *Prog. Polym. Sci.*, **37**: 1510-1551.
3. Bock, N., Woodruff, M. A., Hutmacher, D. W., and Dargaville, T. R. (2011). Electrospaying, a Reproducible Method for Production of Polymeric Microspheres for Biomedical Applications. *Polymers*, **3**: 131-149.
4. Burger, C., Hsiao, B. S., and Chu B. (2006). Nanofibrous materials and their applications. *Annu. Rev. Mater. Sci.*, **36**: 36(1): 333-368.
5. Celebioglu, A., and Uyar, T. (2011). Electrospinning of Polymer-free Nanofibers from Cyclodextrin Inclusion Complexes. *Langmuir*, **27**: 6218-6226.
6. Cipitria, A., Skelton, A., Dargaville, T. R., and Hutmacher, D. W. (2011). Design, fabrication and characterization of PCL electrospun scaffolds-a review. *J. Mater. Chem.*, **21**: 9419-9453.
7. Kostakova, E., Seps, M., Pokorny, P., and Lukas, D. (2014). Study of polycaprolactone wet electrospinning process. *Express Polym. Lett.*, **8**: 554-564.
8. Enayati, M., Ahmad, Z., Stride, E., and Edirisinghe, M. (2010). Size mapping of electric field-assisted production of polycaprolactone particles. *J. R. Soc. Interface*, **7**: S393-S402.
9. Gupta, P., Elkins, C., Long, T. E., and Wilkes, G. L. (2005). Electrospinning of linear homopolymers of poly(methyl methacrylate): exploring relationships between fiber formation, viscosity, molecular weight and concentration in a good solvent. *Polymer*, **46**: 4799-4810.
10. Hohman, M. M., Shin, M., Rutledge, G., and Brenner, M. P. (2001). Electrospinning and electrically forced jets. I. Stability theory. *Phys. Fluids*, **13**: 2201-2220.
11. Hohman, M. M., Shin, M., Rutledge, G., and Brenner, M. P. (2001). Electrospinning and electrically forced jets. II. Applications. *Phys. Fluids*, **13**: 2221-2236.
12. Hubbard, P. L., Zhou, F.-L., Eichhorn, S. J., and Parker, G. J. M. (2015). Biomimetic phantom for the validation of diffusion magnetic resonance imaging. *Magn. Reson. Med.*, **73**: 299-305.

13. Jaworek, A. (2007). Micro- and nanoparticle production by electrospraying. *Powder. Technol.*, **176**: 18-35.
14. Vyslouzilová, L., Valtera, J., Pejchar, K., Beran, J., and Lukas, D. (2014). Design of Coaxial Needleless Electrospinning Electrode with Respect to the Distribution of Electric Field. *Appl. Mech. Mater.*, **693**: 394-399.
15. Labbaf, S., Ghanbar, H., Stride, E., and Edirisinghe, M. (2014). Preparation of Multilayered Polymeric Structures Using a Novel Four-Needle Coaxial Electrohydrodynamic Device. *Macromol. Rapid Comm.*, **35**: 618-623.
16. Li, D., and Xia, Y. (2004). Electrospinning of Nanofibers: Reinventing the Wheel? *Adv. Mater.*, **16**: 1151-1170.
17. Mahalingam, S., Raimi-Abraham, B. T., Craig, D. Q. M., and Edirisinghe, M. (2015). Formation of Protein and Protein-Gold Nanoparticle Stabilized Microbubbles by Pressurized Gyration. *Langmuir*, **31**: 659-666.
18. McHugh, D. J., Zhou, F.-L., Hubbard Cristinace, P. L., Naish, J. H., and Parker, G. J. M. (2015). Ground Truth for Diffusion MRI in Cancer: A Model-Based Investigation of a Novel Tissue-Mimetic Material. in *IPMI 2015 UK Proceedings*. S. Ourselin, C. D. Alexander, C.-F. Westin and J. M. Cardoso. Springer International Publishing, 179-190.
19. Megdi, E., Eleanor, S., and Edirisinghe, M. (2013). Electrospayed core-shell polymer-lipid nanoparticles for active component delivery. *Nanotechnology*, **24**: 465604.
20. Meng, F.Z., Jiang, Y., Sun, Z. H., Yin, Y. Z., and Li, Y. Y. (2009). Electrohydrodynamic liquid atomization of biodegradable polymer microparticles: Effect of electrohydrodynamic liquid atomization variables on microparticles. *J. Appl. Polym. Sci.*, **113**: 526-534.
21. Nukavarapu, S. P., Kumbar, S. G., Brown, J. L., Krogman, N. R., Weikel, A. L., Hindenlang, M. D. Nair, L. S., Allcock, H. R., and Laurencin, C. T. (2008). Polyphosphazene/Nano-Hydroxyapatite Composite Microsphere Scaffolds for Bone Tissue Engineering. *Biomacromolecules*, **9**: 1818-1825.
22. Park, C. H. and Lee, J. (2009). Electrospayed polymer particles: Effect of the solvent properties. *J. Appl. Polym. Sci.*, **114**: 430-437.
23. Teo, W. E. and Ramakrishna, S. (2006). A review on electrospinning design and nanofibre assemblies. *Nanotechnology*, **17**: R89.
24. Sharma, U., Pham, Q., Marini, J., Yan, X., and Core, L. (2012). Electrospinning Process for Manufacture of Multi-Layered Structures. US patent, Application number US 13/362,467.
25. Van der Schueren, L., De Schoenmaker, B. Kalaoglu, O. I., and De Clerck, K. (2011). An alternative solvent system for the steady state electrospinning of polycaprolactone. *Euro. Polym. J.*, **47**: 1256-1263.
26. Guarino, V., Khodir, W. K., and Ambrosio, L. (2012). Biodegradable microparticles and nanoparticles by electrospraying techniques. *J. Appl. Biomater. Funct. Mater.*, **10**: 191-196.
27. Woodruff, M. A. and Hutmacher, D. W. (2010). The return of a forgotten polymer - Polycaprolactone in the 21st century. *Prog. Polym. Sci.*, **35**: 1217-1256.
28. Wu, Y. and Clark, R. L. (2007). Controllable porous polymer particles generated by electrospraying. *J. Colloid Interf. Sci.*, **310**: 529-535.
29. Qin, X. H. and Jiang, G. J. (2014). High-efficiency needleless coaxial electrostatic spinning device and method. Chinese patent, application number CN 201310586614.
30. Xie, J., Marijnissen J. C. M., and Wang, C.-H. (2006). Microparticles developed by electrohydrodynamic atomization for the local delivery of anticancer drug to treat C6 glioma in vitro. *Biomaterials*, **27**: 3321-3332.
31. Xu, Y. and Hanna, M. A. (2006). Electro spray encapsulation of water-soluble protein with polylactide: Effects of formulations on morphology, encapsulation efficiency and release profile of particles. *Int. J. Pharm.*, **320**: 30-36.
32. Yan, X., Marini, J., Mulligan, R., Deleault, A., Sharma, U., Brenner, M. P., Rutledge, G. C., Freyman, T., and Pham. Q. P. (2015). Slit-Surface Electrospinning: A Novel Process Developed for High-Throughput Fabrication of Core-Sheath Fibers. *PLoS ONE* **10**: e0125407.
33. Yao, J., Kuang Lim, K., Xie, J. W., Hua, J., and Wang, C.-H. (2008). Characterization of electrospraying process for polymeric particle fabrication. *J. Aerosol. Sci.*, **39**: 987-1002.
34. Yu, L., Ni, C., Grist S., Bayly, C., and Cheung, K. (2015). Alginate core-shell beads for simplified three-dimensional tumor spheroid culture and drug screening. *Biomed. Microdevices*, **17**: 1-9.
35. Zhou, F.-L., Hubbard, P. L., Eichhorn, S. J., and Parker, G. J. M. (2011). Jet deposition in near-field electrospinning of patterned polycaprolactone and sugar-polycaprolactone core-shell fibres. *Polymer*, **52**: 3603-3610.

